Environmental Science & Technology

pubs.acs.org/est

Article

Using Mercury Stable Isotopes to Quantify Directional Soil−Atmosphere Hg(0) Exchanges in Rice Paddy Ecosystems: Implications for Hg(0) Emissions to the Atmosphere from Land Surfaces

Kun Zhang, Qiang Pu, Jiang Liu, Zhengdong Hao, Lijuan Zhang, Leiming Zhang, Xuewu Fu, Bo Meng,* and Xinbin Feng

Cite This: *Environ. Sci. Technol.* 2024, 58, 11053−11062

Read Online

ACCESS | Metrics & More | Article Recommendations | Supporting Information

ABSTRACT: Gaseous elemental mercury [Hg(0)] emissions from soils constitute a large fraction of global total Hg(0) emissions. Existing studies do not distinguish biotic- and abiotic-mediated emissions and focus only on photoreduction mediated emissions, resulting in an underestimation of soil Hg(0) emissions into the atmosphere. In this study, directional mercury (Hg) reduction pathways in paddy soils were identified using Hg isotopes. Results showed significantly different isotopic compositions of Hg(0) between those produced from photoreduction (δ^{202}Hg = −0.80 ± 0.67‰, Δ^{199}Hg = −0.38 ± 0.18‰), microbial reduction (δ^{202}Hg = −2.18 ± 0.25‰, Δ^{199}Hg = 0.29 ± 0.38‰), and abiotic dark reduction (δ^{202}Hg = −2.31 ± 0.25‰, Δ^{199}Hg = 0.50 ± 0.22‰). Hg(0) exchange fluxes between the atmosphere and the paddy soils were dominated by emissions, with the average flux ranging from 2.2 ± 5.7 to 16.8 ± 21.7 ng m^{-2} h^{-1} during different sampling periods. Using an isotopic signature-based ternary mixing model, we revealed that photoreduction is the most important contributor to Hg(0) emissions from paddy soils. Albeit lower, microbial and abiotic dark reduction contributed up to 36 ± 22 and 25 ± 15%, respectively, to Hg(0) emissions on the 110th day. These novel findings can help improve future estimation of soil Hg(0) emissions from rice paddy ecosystems, which involve complex biotic-, abiotic-, and photoreduction processes.

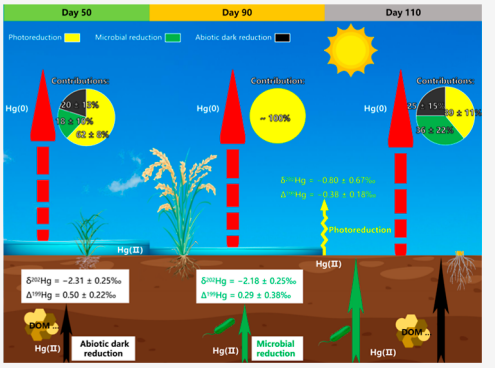

KEYWORDS: *mercury reduction, mercury stable isotope, rice paddy, mercury emission*

1. INTRODUCTION

Mercury (Hg) is a pollutant of global concern due to its persistence, neurotoxicity, and bioaccumulation.[1] Gaseous elemental mercury [Hg(0)] is the most abundant form of Hg in the atmosphere and can be transported regionally and globally due to its extended atmospheric residence time (>0.5 years).[2,3] Atmospheric Hg(0) is released via both anthropogenic (e.g., mining and fossil fuel combustion) and natural sources (e.g., hydrothermal and volcanic activities, biomass burning).[4] Recent estimates of Hg emissions from anthropogenic sources are reasonably accurate, whereas those from natural sources still have large uncertainties[5,6] due to a limited understanding of the air-surface Hg(0) exchange processes over different land uses.[4]

Given that terrestrial soils are the largest reservoir for natural and legacy anthropogenic Hg, accurately estimating global soil emissions is critical for assessing global Hg cycling.[7,8] The 2018 Global Mercury Assessment showed that Hg(0) emissions from soil and vegetation accounted for 48% of natural Hg emissions from terrestrial ecosystems.[1] Photoreduction, microbial reduction, and abiotic dark reduction are considered the primary processes contributing to Hg(0) emissions from soils.[9] Solar radiation was considered the dominant factor for Hg reduction;[10−12] therefore, soil Hg(0) emissions are primarily assessed based on the photoreduction process in chemical transport models.[2,13,14] Considering that microbial and abiotic dark reduction processes of Hg in the environment have been widely reported,[9,15,16] neglecting these processes could result in an underestimation of soil Hg(0) emissions. For example, in forest soils, microbial and abiotic dark reduction processes contribute even more to soil Hg(0) emissions than does the photoreduction process.[9,15]

Wetlands play an important role in global Hg cycling and have become a net source of atmospheric Hg(0) due to

Received: February 29, 2024
Revised: June 4, 2024
Accepted: June 5, 2024
Published: June 13, 2024

https://doi.org/10.1021/acs.est.4c02143
Environ. Sci. Technol. 2024, 58, 11053−11062

declining atmospheric Hg concentrations.[17] Rice paddies are the largest human-made wetlands and account for approximately 18% of the global total wetlands.[18] Hg(II) reduction through photoreduction, microbial reduction, and abiotic dark reduction processes can lower the concentration of substrates available for Hg-methylation, and is thus a critical step of Hg cycling in paddy soils.[19−21] However, the relative importance of the above-mentioned reduction processes for Hg(0) emissions from paddy soils remains elusive, mainly due to traditional observations of Hg(0) concentration and exchange flux not being able to distinguish Hg(0) emitted from different reduction processes.

Mercury isotope geochemistry is a useful tool for tracing and quantifying the sources and biogeochemical pathways of Hg in natural environments.[22−24] A prerequisite of this approach is to obtain Hg isotopic compositions from different sources. Degrees of mass-dependent fractionations (MDF, expressed as δ^{202}Hg) and mass-independent fractionations (MIF, expressed as Δ^{199}Hg) were determined for various biotic and abiotic processes.[22] Previously, isotopic fractionation signatures of Hg(II) reduction processes were detected based on indoor experiments instead of field conditions.[25−29] For microbial Hg(II) reduction processes, while the experiments showed an MDF, the degree of Hg isotope fractionation varied greatly [e.g., the enrichment factor (ε^{202}Hg) ranged from −2.00 to −1.20‰] as a result of differences in microbial Hg(0) reduction capacity and experimental conditions.[26,27] Similarly, due to inconsistent experimental conditions, large ranges of MDF and MIF were observed in photoreduction experiments with ε^{202}Hg ranging from −1.72 to −0.60‰ and E^{199}Hg ranging from −6.73 to −0.43‰.[25,28,30−32] In abiotic dark reduction experiments, ε^{202}Hg ranged from −2.20 to −1.52‰ and E^{199}Hg ranged from 0.17 to 0.26‰.[28,29,33,34] Large uncertainties still exist in evaluating the contributions of various reduction processes to Hg(0) emissions from rice paddies using the Hg(0) isotopic compositions detected from the above-mentioned Hg(II) reduction experiments.

To address the issues summarized above, we conducted field studies followed by laboratory analysis to (1) determine Hg isotope fractionation of microbial reductions, photoreductions, and abiotic dark reductions, (2) characterize exchange fluxes and isotopic compositions of Hg(0) in the atmosphere−paddy soil exchange process using a dynamic flux chamber (DFC), and (3) quantify the relative contributions of different Hg(II) reduction processes to Hg(0) emissions from paddy soils. Results from this study broaden the current understanding of the complex soil−atmosphere Hg(0) exchange processes in croplands and provide high-quality data supporting future estimates of natural Hg(0) emissions.

2. MATERIALS AND METHODS

2.1. Study Area and Sampling Site. Field experiments were performed in a rice paddy (Gouxi, 109°11′27″ E, 27°33′48″ N) located in the Wanshan Hg mining area in Guizhou Province, southwestern China. Gouxi was once one of the largest artisanal Hg mining centers in China.[35] Although large-scale Hg mining activities in the Wanshan Hg mining area ceased in 2003, Hg concentrations in the air (37.3−416 ng m^{-3}[36]) were consistently higher than the background value in Guizhou (2.8−8.2 ng m^{-3}[36]). Previous studies reported that, in addition to significant methylation processes, the Hg(II) reduction process was also active in paddy soils in this study area,[19−21] which may be the main cause for the consistently high atmospheric Hg(0) concentrations. Therefore, this artisanal Hg mining site was selected for examining soil−atmosphere Hg(0) flux exchanges. The average total Hg and MeHg concentrations in paddy soils were 17.2 ± 1.7 mg kg^{-1} and 2.42 ± 1.6 μg kg^{-1}, respectively.[20,37] The average soil organic matter in the paddy soils was 8 ± 1.2%.[37] The average pH of the paddy soils was 7.0 ± 0.6,[37] which is comparable to or even lower than that in the higher Hg-contaminated soil (7.2 ± 0.8) or the background soil (7.4 ± 0.2) from different locations in China.[37] The redox potential measured under flooded conditions in the rice paddy was 106.0 ± 26.3 mV.

2.2. Design of the Indoor and Field Experiments. This study conducted indoor and field experiments to obtain Hg isotopic fractionation characteristics of different reduction processes, the isotopic compositions of the product Hg(0), and Hg(0) exchange fluxes between the atmosphere and paddy soils. All the experimental designs are described in detail below.

2.2.1. Isotopic Fractionation during the Microbial Reduction of Hg(II). The bacterial strain selected for this study was *Geobacter sulfurreducens* (*G. sulfurreducens*) PCA, which is a ubiquitous iron-reducing bacterium found in various ecosystems, including rice paddies.[38,39] We have previously detected a high abundance of *G. sulfurreducens* PCA (accounting for 0.3% of the total bacteria population), which is the dominant Hg-reducing microorganism in the investigated paddy soils.[40] Therefore, it is reasonable to use *G. sulfurreducens* PCA to study isotope fractionation during the process of microbial reduction of Hg(II). The quality control details of the microbial reduction experiment are described in Text S1.

In the pre-experiment, dissolved organic matter (DOM) present in the overlying water of the rice paddy cannot be removed by filtering through a 0.22 μm filter (Longjing, China). DOM was reported to be capable of reducing Hg(II) in the dark.[29] Therefore, deionized water (Milli-Q, Millipore, USA) was used in this experiment. In pure culture experiments, the growth conditions of the PCA strain have been previously described.[41] Briefly, the strains were inoculated at 2% (*v*/*v*) in 200 mL of medium and cultured in an anaerobic bottle at 33 °C in the dark (Figure S1). The PCA cells were collected at the exponential growth phase (∼110 h), placed in a 2 mL sterilized centrifuge tube, centrifuged at 1500*g* for 10 min, and subsequently resuspended in phosphate buffer (PBS). The cells were separated equally into 33 anaerobic culture tubes (reactors, volume: 30 mL) after washing three times in PBS and left to stand for 2 h before use in the Hg(II) reduction experiment. PBS was used as the reaction substrate. To obtain enough Hg for concentration and isotope analyses, 33 reactors with 10 mL of PBS were spiked with a NIST-3133 Hg(II) standard to reach an initial Hg(II) concentration of 20 ppb, according to the Hg tolerance curves of *G. sulfurreducens* PCA (Figure S2) (more details are presented in Text S1), and were placed in an oscillation incubator (THZ-98C, Yiheng, China) at a constant temperature of 33 °C.

Anaerobic tubes were sampled for Hg isotope analyses at 0, 12, 16, 20, 24, 28, 32, 36, 40, 44, and 48 h after the experiment was initiated, using the sampling method shown in Figure S1 and described in a previous study.[42] Specifically, three anaerobic culture tubes were removed as parallel samples at each sampling time. The Hg(0) product in the anaerobic culture tubes was purged and preconcentrated into 5 mL of reverse aqua regia (40%, *v*/*v*, HNO_3/HCl = 3:1) by Hg-free

https://doi.org/10.1021/acs.est.4c02143
Environ. Sci. Technol. 2024, 58, 11053−11062

N_2 at a flow rate of 100 mL min^{-1} for 3 h. After purging, excess BrCl was added to the remaining solution to reach a concentration of 2.5% (*v*/*v*) to oxidize the remaining Hg in the anaerobic culture tubes to Hg(II). After >24 h of oxidation, 100 μL of $NH_2OH{\cdot}HCl$ (25%, *w*/*v*) was added to the anaerobic culture tubes to deplete excess BrCl, followed by the addition of 1 mL of $SnCl_2$ solution (20%, *w*/*v*) to reduce the remaining Hg(II) to Hg(0). Similar to the preconcentration procedure mentioned above, the remaining Hg(II) was obtained via preconcentration into 5 mL of 40% reverse aqua regia by Hg-free N_2 at a flow rate of 100 mL min^{-1} for 2 h. The formed Hg(II) samples were sealed and stored at 4 °C in the dark for total Hg concentration and isotope analyses.

2.2.2. Isotopic Fractionation during Photoreduction and Abiotic Dark Reduction of Hg(II). As shown in Figure S3, in situ photoreduction and abiotic dark reduction of Hg(II) were performed in the field from 10th to 13th of July, 2023. To eliminate the effects of microorganisms, cells in the overlying water of the rice paddy were removed using a 0.22 μm filter.[41,43,44] The Hg concentration in the filtered overlying water was 6.9 ± 1.6 ng L^{-1}, and the average Hg isotopic composition was δ^{202}Hg = −0.67 ± 0.21‰, Δ^{199}Hg = 0.29 ± 0.38‰ (2SD).[45] Prior to the experiment, the filtered overlying water was divided into two precleaned polyethylene (PE) boxes (~30 L) with the water level above the edge of the DFC to isolate ambient air. The matched open top size of the PE box (45 × 32 cm) with the exchange area of DFC (30 × 30 cm) was designed to minimize evaporation. An air scrubber (Zero canister, Tekran) at the inlet of DFC was used as a source of Hg-free air.[46] Hg(0) samples were collected from the DFC outlet using a chlorine-impregnated activated carbon (CLC, mass: 0.6 g) trap with a flow rate of 1.0−2.0 L min^{-1}.[47] Two sets of experiments were conducted simultaneously with two DFC systems. During the day, the DFCs were exposed to natural sunlight to collect Hg(0) samples produced from the photoreduction process, while at night, the DFCs were covered by light-tight boxes to collect Hg(0) samples produced from the abiotic dark reduction process. During the experiment, 5 L of sterile overlying water was replaced every 6 h in the PE box to simulate the dynamic balance of Hg in the overlying water. Each Hg(0) sample collected from the DFC outlet represents a 12 h mixed sample under net emission conditions. During the 4 day sampling period, eight batches of samples were collected, with two parallel samples collected simultaneously in each batch. Eight Hg(0) samples were collected during the day and eight were collected during the night. After completing the sampling, the CLC traps were plugged with Teflon stoppers and sealed with three clean polyethylene bags, stored in the dark, and shipped to the laboratory.

In the laboratory, the Hg(0) samples were preconcentrated from the CLC traps into 5 mL of 40% reverse aqua regia solution using the thermal desorption method.[48] The trapping solutions were stored in brown glass bottles at 4 °C in the dark before Hg concentration and isotopic composition analyses.

2.2.3. Hg0 Flux and Isotopic Compositions from Paddy Soil−Atmosphere Exchange. In 2021, Hg(0) exchange flux between the paddy soil and the atmosphere was measured at Gouxi using the DFC method (Figure S4).[36,49] Sampling was performed on the 50, 90, and 110th day after transplanting and first flooding, with each sampling period lasting 24 h. Given the significant impacts of flooding and solar radiation on Hg(0) emissions from paddy soils,[57,58] day 50 and 90th were selected to assess the variations in Hg(0) emissions under different solar radiation intensities. Additionally, day 110th was chosen for sampling to examine the changes in soil Hg(0) emissions between flooded and dry conditions. During the field sampling, the soil temperature, soil moisture, and solar radiation were recorded by an in situ single-layer soil moisture temperature tester (TPFS-WS-1, Shanghai, China) and an automatic meteorological station (misol HP2000, China). Soil moisture (dry basis water content: described by the percentage equivalent of the ratio of the weight of water to the weight of the dry soil) at a depth of 1 cm was 92 ± 8% on the 50th day, 102 ± 16% on the 90th day, and 15 ± 0.8% on the 110th day. Under flooded conditions, the soil temperatures on the 50 and 90th day were 25.2 ± 1.0 and 28.0 ± 1.1 °C, respectively. Regarding the maximum solar radiation, the different stages decreased in the order of 90th day (748 W m^{-2}) > 110th day (615 W m^{-2}) > 50th day (405 W m^{-2}). Hg(0) samples from the DFC inlet and outlet were collected simultaneously using CLC traps with a flow rate of 1.0−2.0 L min^{-1}. The CLC traps in the DFC inlet and outlet were replaced every 6 h, i.e., each CLC trap represented a 6 h mixed sample. Twelve Hg(0) samples were collected from the DFC inlet and outlet, respectively. The CLC traps were plugged with Teflon stoppers and sealed with three clean polyethylene bags, stored in the dark, and shipped to the laboratory for Hg concentration and isotopic composition analyses. Detailed sample information is shown in Table S3.

2.3. Chemical Analysis of Hg(0) and Hg(II) Concentrations and Isotopic Compositions. All CLC traps were preconcentrated into 5 mL of oxidizing solution of 40% reverse aqua regia using a tube muffle furnace.[46] Hg concentrations in the product and reactant trapping solutions were determined by $SnCl_2$ reduction and cold vapor atomic fluorescence spectrophotometry (CVAFS, Brooks Rand) according to US EPA 1631.[50] During the analysis of Hg concentrations, the standard reference material (GBW07405) was treated in the same manner as for the CLC samples using the thermally desorbed method, with a Hg recovery of 100 ± 14% (1SD, *n* = 7).

The concentrations of Hg in the trapping solutions were diluted to 0.5−1 ng mL^{-1} for isotope analysis using a Nu-Plasma II multicollector inductively coupled plasma−mass spectrometer (MC-ICP-MS).[51] The NIST-3133 Hg standard solution was prepared at 0.5−1 ng mL^{-1} Hg in 10% HCl (*v*/*v*) and measured as a bracketing Hg standard in the same manner as the test samples. The MDF of the Hg isotope is expressed using the δ^{xxx}Hg notation with reference to NIST-3133 (analyzed before and after every two samples) in accordance with eq 1

$$\delta^{xxx}\mathrm{Hg}(‰) = [(^{xxx}\mathrm{Hg}/^{198}\mathrm{Hg})_{\mathrm{sample}} / (^{xxx}\mathrm{Hg}/^{198}\mathrm{Hg})_{\mathrm{NIST-3133}} - 1] \times 1000 \quad (1)$$

where *xxx* represents the mass number of Hg isotopes (199, 200, 201, and 202).[25] The MIF is expressed using the capital delta notation (Δ^{xxx}Hg) and calculated as eq 2[25]

$$\Delta^{xxx}\mathrm{Hg}(‰) = \delta^{xxx}\mathrm{Hg} - (\beta_{xxx} \times \delta^{202}\mathrm{Hg}) \quad (2)$$

where the corresponding scaling factors β_{xxx} are 0.2520, 0.5024, and 0.7520 for ^{199}Hg, ^{200}Hg, and ^{201}Hg, respectively.

During the analysis of Hg isotopic compositions, NIST-8610 secondary standard solutions were analyzed once after every 10 samples. The average and uncertainty of the Hg isotopic

https://doi.org/10.1021/acs.est.4c02143
Environ. Sci. Technol. 2024, 58, 11053−11062

compositions of NIST-8610 (δ^{202}Hg = −0.53 ± 0.07‰, Δ^{199}Hg = 0.00 ± 0.06‰, Δ^{200}Hg = 0.00 ± 0.08‰, Δ^{201}Hg = −0.03 ± 0.06‰, 2SD, n = 14) agree well with previous studies.[52,53]

2.4. Data Analysis. *2.4.1. Mercury Mass Balance, Isotopic Balance, and Isotope Fractionation Characteristics in Microbial Reductions.* The Hg mass and isotopic balances were calculated during the microbial reduction experiment to assess the quality of the data. Given that the experimental system was closed, the sum of the Hg content and the Hg isotopes in the products and reactants during these processes should be consistent with the initial addition of Hg(II). Detailed calculation methods are provided in Text S2.

2.4.2. Calculation of the Hg(0) Exchange Flux Between the Atmosphere and Paddy Soils. Hg(0) exchange fluxes (F, ng m^{-2} h^{-1}) between the atmosphere and paddy fields were calculated using the following equation

$$F = \frac{Q}{A} \times (C_o - C_i) \tag{3}$$

where C_o and C_i represent the Hg(0) concentrations (ng m^{-3}) in the DFC outlet and inlet air, respectively, Q is the flow rate through the DFC (m^3 h^{-1}), and A is the area enclosed by the DFC (0.09 m^2).

2.4.3. Hg(0) Isotopic Compositions during the Paddy Soil−Atmosphere Exchange. MDF ($\delta^{202}Hg_{ex}$) and MIF ($\Delta^{199}Hg_{ex}$, $\Delta^{201}Hg_{ex}$) signatures for paddy soil−atmosphere Hg(0) exchanges were calculated following the method described by Zhu et al.[36] Given the potential simultaneous occurrence of emission and deposition of Hg(0) in DFC, a modification factor (CMF) (ratio of $(C_o - C_i)/C_o$) based on the analytical uncertainty of Hg(0) concentrations was used to separate cases with significant Hg(0) emission (CMF > 0.15) and deposition (CMF < − 0.15).[36] The detailed information on the calculation method can be found in Text S3.

2.4.4. Source Apportionment Analysis. Based on the isotopic compositions of the product Hg(0) of the three main reduction processes (photoreduction, microbial reduction, and dark abiotic reduction) in paddy soils, a triple mixing model was constructed to evaluate the relative contributions of the three processes to Hg(0) emissions from paddy fields using eqs 4−6

$$\delta^{202}Hg_s = \delta^{202}Hg_p \times F_p + \delta^{202}Hg_d \times F_d + \delta^{202}Hg_m \times F_m \tag{4}$$

$$\Delta^{199}Hg_s = \Delta^{199}Hg_p \times F_p + \Delta^{199}Hg_d \times F_d + \Delta^{199}Hg_m \times F_m \tag{5}$$

$$F_p + F_d + F_m = 1 \tag{6}$$

where δ^{202}Hg and Δ^{199}Hg with the subscripts s, p, d, and m represent the isotopic composition of Hg(0) emitted from paddy soils, Hg(0) produced from photoreduction, dark abiotic reduction, and microbial reduction, respectively. F_p, F_d, and F_m are the contribution rates of Hg(0) produced from the three reduction processes.

The uncertainties in the isotopic compositions of Hg(0) produced from microbial reduction and dark abiotic reduction were quantified through Monte Carlo simulations. The isotopic compositions of Hg(0) produced from photoreduction were obtained by measurements (see Section 3.2). In the Hg isotopic mixing model, a sample size of 100,000 isotopic compositions of Hg(0) produced from different processes was selected randomly for model simulation using eqs 4−6. The Monte Carlo simulations were completed using the MATLAB program, and the source code is shown in Text S4.

2.5. Quality Control and Statistical Analysis. During the analysis of Hg concentrations, the standard reference material (GBW07405) was treated in the same manner as for the CLC samples using the thermally desorbed method, with a Hg recovery of 100 ± 14% (1SD, n = 7). During the experiment on the microbial reduction of Hg(II), the sum of the product Hg(0) and the reactant Hg(II) remaining in the buffer, as calculated using eq S1 (Text S2), showed a 94.3 ± 15.1% (2SD) of mass balance (Figure S5). The total Hg isotopic compositions calculated using eqs S2 and S3 in Text S2 (δ^{202}Hg = −0.03 ± 0.10‰ and Δ^{199}Hg = −0.01 ± 0.06‰, 2SD, n = 27) were highly consistent with the isotopic compositions of the initially added Hg(II) standard (NIST-3133) (Figure S6).

The data was plotted using Origin Pro 2018. Group differences were assessed using t-tests and one-way ANOVAs with Duncan's post hoc tests using SPSS Statistics 24 for Windows. Statistical significance (p) was set at <0.05 (two-tailed).

3. RESULTS AND DISCUSSION

3.1. Mercury Isotope Fractionation Characteristics during the Microbial Reduction of Hg(II). With progression of the experiment of Hg (II) reduction by bacteria, the proportion of Hg(II) in the reactant gradually decreased, while that of Hg(0) in the product gradually increased (Table S1). The product Hg(0), expressed as the percentage of the initially added Hg(II), reached a maximum value of ∼80% 44 h after initiation of the experiment (Figure S5). As described in Section 2.5, the Hg mass (94.3 ± 15.1%) and isotopes (δ^{202}Hg = −0.03 ± 0.10‰ and Δ^{199}Hg = −0.01 ± 0.06‰) followed a mass balance throughout the experiment, indicating the reliability of the experimental design and results (Figures S5 and S6). The product Hg(0) represented a lower δ^{202}Hg than did the reactant Hg(II) (Figure 1), indicating that *G. sulfurreducens* PCA preferentially reduced the lighter isotopes of Hg as the reaction progressed. As shown in Table S1 and Figure S6, the reduction process resulted in a negative δ^{202}Hg shift (up to −1.60‰) between the product Hg(0) and the initially added Hg(II), and a positive δ^{202}Hg shift (up to 1.50‰) between the reactant Hg(II) and the initially added Hg(II). However, Δ^{199}Hg of product Hg(0) and reactant Hg(II) were 0.04 ± 0.14‰ and −0.02 ± 0.10‰, respectively (2SD, n = 27), which were not significantly different (p > 0.05) from Δ^{199}Hg of the initial added Hg(II) (Figure 1).

During the microbial reduction experiment, the reactor can be regarded as a relatively closed system experiment. Consequently, the reactant Hg(II) and the product Hg(0) were re-equilibrated, and the initial kinetic fractionation was overprinted by isotope exchange.[33,34,54] As shown in Figure 1, both the product Hg(0) and the reactant Hg(II) followed a linear equilibrium fractionation model with experimental progression. Given that the sum of the squared residuals of the linear fit for the product Hg(0) (0.81) was smaller than that for the reactant Hg(II) (1.78), the Hg isotope enrichment factor (ε^{202}Hg) was −1.51 ± 0.24‰ (2SD). This value falls within the range previously reported (ε^{202}Hg range from −1.20 ± 0.10 to −2.00 ± 0.20‰, 2SD).[26,27]

https://doi.org/10.1021/acs.est.4c02143
Environ. Sci. Technol. 2024, 58, 11053−11062

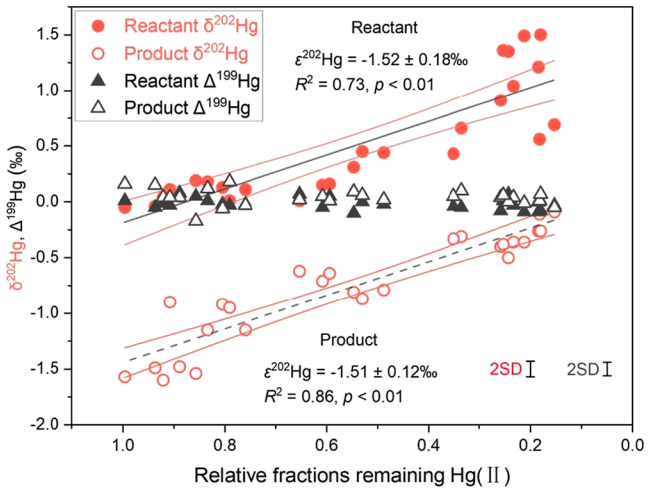

Figure 1. Hg stable isotope fractionation of reactant Hg(II) and product Hg(0) for δ^{202}Hg (MDF) and Δ^{199}Hg (MIF). Linear equilibrium model fits based on reactant Hg(II) and product Hg(0) are represented by solid and dashed lines, respectively. The envelopes represent the 95% confidence intervals. The error bars represent ±2 standard deviations for the δ^{202}Hg and Δ^{199}Hg of NIST-8610.

3.2. Mercury Isotope Fractionation during Photoreduction and Abiotic Dark Reduction Processes in Rice Paddies. Hg concentrations and isotopic compositions of the filtered overlying water during the experiment were calculated using a Hg mass and isotopic balance model (Text S5). The results showed that the Hg concentration in the overlying water before sampling in batches 2−8 was 6.3 ± 0.4 ng L^{-1} (1SD, n = 7), which was comparable (p > 0.05) to the Hg concentration in the initial overlying water (6.9 ± 1.6 ng L^{-1}). Similarly, the Hg isotopic composition (δ^{202}Hg = −0.71 ± 0.14‰, Δ^{199}Hg = 0.33 ± 0.03‰, 2SD, n = 7) of the overlying water before sampling in batches 2−8 was also not significantly (p > 0.05) different from the Hg isotopic composition (δ^{202}Hg = −0.67 ± 0.21‰, Δ^{199}Hg = 0.29 ± 0.38‰[45]) at the beginning. The isotopic signatures of the product Hg(0) during the in situ Hg(II) photoreduction and abiotic dark reduction processes are shown in Table S2. The Hg(0) collected from the DFC outlet during daytime had a δ^{202}Hg of −0.80 ± 0.67‰ and Δ^{199}Hg of −0.38 ± 0.18‰ (2SD, n = 8). The Hg(0) from the DFC outlet during nighttime had a δ^{202}Hg of −0.79 ± 0.57‰ and Δ^{199}Hg of −0.32 ± 0.32‰ (2SD, n = 8). Additionally, the isotopic signatures of the outlet Hg(0) collected during the day showed a Δ^{199}Hg/Δ^{201}Hg ratio of 1.07 ± 0.22 (R^2 = 0.80, p < 0.01, Figure S7), implying that the emitted Hg(0) exhibited a signature of photoreduction.[25] The isotopic data of Hg(0) collected at night did not show a significant correlation (p > 0.05), and were in the opposite direction of MIF according to the results of the abiotic dark reduction experiments.[29] Abiotic dark reduction of Hg(II) generally produces a small positive odd-MIF shift in the product Hg(0).[29] However, the average isotopic compositions of the Hg(0) collected from the DFC outlet at night were similar to those collected during the day, as seen from the signature values presented above. This phenomenon may be because very little abiotic dark reduction occurs at night, and a

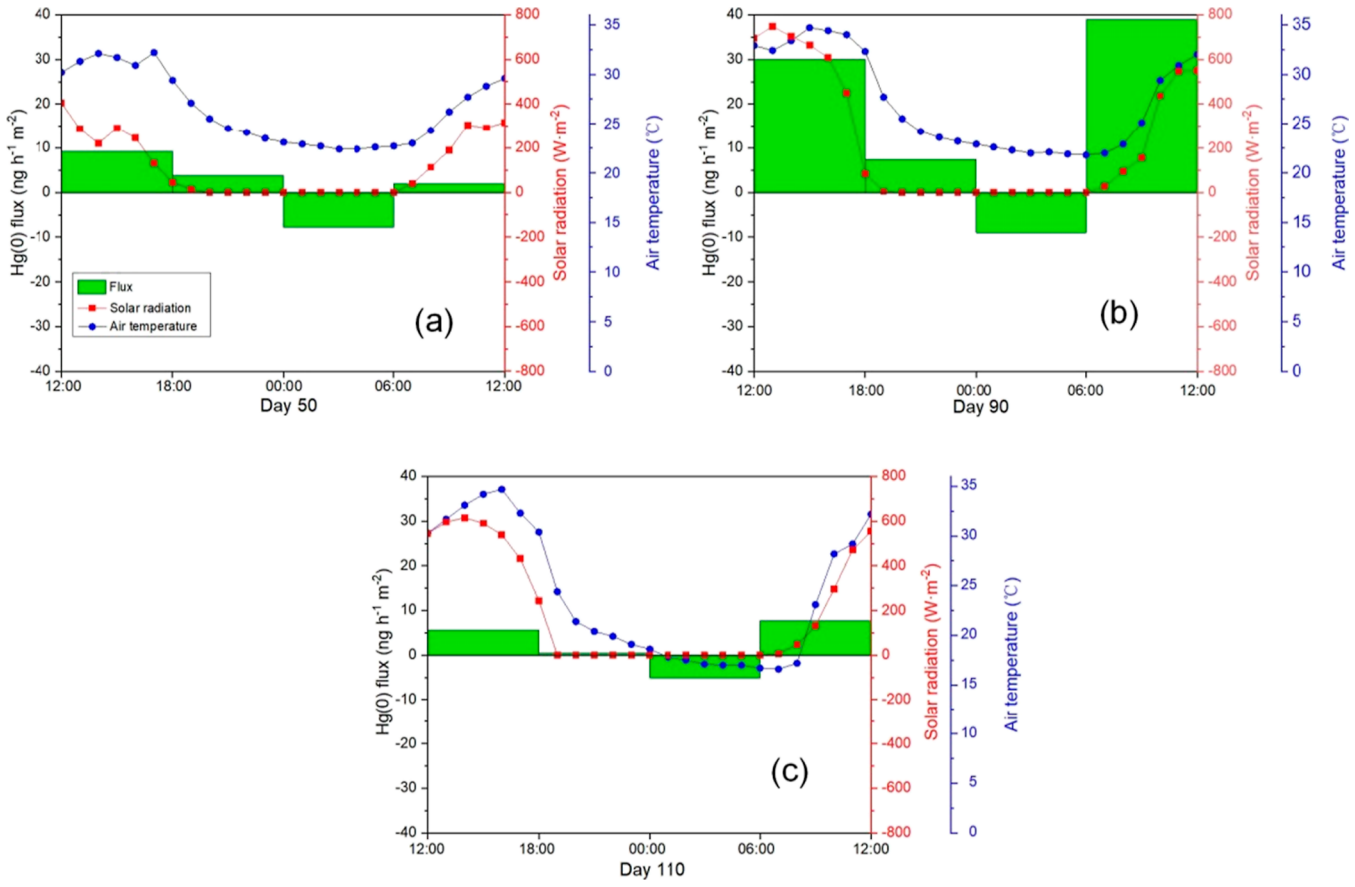

Figure 2. Diurnal variations of atmosphere−paddy soil Hg(0) exchange fluxes and meteorological parameters.

https://doi.org/10.1021/acs.est.4c02143
Environ. Sci. Technol. 2024, 58, 11053−11062

delayed release of Hg(0) was previously produced during the day.[49] Therefore, Hg(0) collected at night cannot be used as an endmember for abiotic dark reduction in the mixing model.

3.3. Atmosphere−Paddy Soil Hg(0) Exchange Fluxes. The average (±1SD) Hg(0) fluxes between the paddy soils and the atmosphere on the 50, 90, and 110th day were 5.6 ± 10.8 ng m^{-2} h^{-1} (range: − 7.8 to 18.4 ng m^{-2} h^{-1}), 16.8 ± 21.7 ng m^{-2} h^{-1} (−9.0 to 38.8 ng m^{-2} h^{-1}), and 2.2 ± 5.7 ng m^{-2} h^{-1} (−5.1 to 7.7 ng m^{-2} h^{-1}), respectively (Figure 2). Hg(0) emissions dominated the Hg(0) exchange fluxes between the atmosphere and the paddy soils, especially during daytime. The soils were not a significant sources of Hg(0), and were even a sink (flux < 0) of atmospheric Hg(0) during nighttime. In addition, there was no significant difference (p > 0.05) in the average (±1SD) daytime temperatures on the 50th (29.0 ± 3.0 °C), 90th (30.5 ± 4.4 °C), and 110th day (28.7 ± 6.0 °C). This phenomenon has also been observed in many other vegetated canopies,[55] highlighting the role of solar radiation on Hg(0) emissions.

It is noted that soil Hg(0) emission fluxes were significantly higher on the 90th than the 50th and 110th day (p < 0.01) (Figure 2). The stronger solar radiation on the 90th than 50th day likely played an important role in the higher Hg(0) emission on the 90th day through sunlight-induced processes (photoreduction and volatilization) that reduced Hg(II) to Hg(0) in rice paddy soils.[56,57] The change in paddy soils from flooding to drying on the 110th day was possibly the main reason for the decreased Hg(0) emissions, since exchange fluxes between the soil and atmosphere can be minimized by low soil porosity in dry paddy soils.[21,58] In addition, low penetration of solar radiation and a relatively aerobic environment could limit photoreduction and relevant biotic activities in dry paddy soils, resulting in low diffusion of Hg(0) to the atmosphere.[21,58] As shown in Table S3, the inlet Hg(0) concentration on the 90th day (54.7 ± 11.2 ng m^{-3}) was significantly greater (p < 0.01) than that on the 50th day (15.5 ± 3.6 ng m^{-3}) and 110th day (8.9 ± 2.4 ng m^{-3}), indicating that the overall Hg(0) concentration in ambient air seems to be related to solar radiation.

3.4. Estimation of the Contributions of Different Hg(II) Reduction Processes to Hg(0) Emissions from Rice Paddy Soils. Given that this study focused mainly on the emission of Hg(0) from paddy soils, only the samples with a CMF > 0.15 for the released Hg(0) isotopes are discussed here (Table S3). During the period of investigation, the mean isotopic compositions of Hg(0) collected from the DFC outlet and inlet were δ^{202}Hg = −0.48 ± 0.60‰, Δ^{199}Hg = −0.03 ± 0.15‰ (2SD, n = 7) and δ^{202}Hg = 0.00 ± 0.67‰, Δ^{199}Hg = 0.04 ± 0.08‰ (2SD, n = 7), respectively. The δ^{202}Hg of Hg(0) at the outlet was more negative than that at the inlet (p < 0.05), which may be caused by the emissions of Hg(0) from the paddy soil to the air.[46] The Δ^{199}Hg of Hg(0) at the outlet was not significantly different (p > 0.05) from that at the inlet. This finding is consistent with the results of a previous study in the Wanshan.[36] Under net emission conditions, the mean Hg(0) isotopic compositions from the paddy soil−atmosphere exchange, as calculated using eqs S4 and S5 (Text S3), were as follows: $\delta^{202}Hg_{ex}$ = −1.22 ± 0.46‰ and $\Delta^{199}Hg_{ex}$ = −0.08 ± 0.20‰ (2SD, n = 3) on the 50th day, $\delta^{202}Hg_{ex}$ = −0.81 ± 0.65‰ and $\Delta^{199}Hg_{ex}$ = −0.45 ± 0.08‰ (2SD, n = 2) on the 90th day, and $\delta^{202}Hg_{ex}$ = −1.54 ± 1.07‰ and $\Delta^{199}Hg_{ex}$ = 0.06 ± 0.10‰ (2SD, n = 2) on the 110th day. These different Hg(0) isotopic compositions (especially odd−MIF) imply differences in reduction processes in paddy soils during the three sampling periods. This is because only photochemical processes can produce significant odd−MIF and abiotic dark reduction only produces small positive odd−MIF, whereas microbial reduction does not produce odd-MIF.[25−29]

The average Hg isotopic compositions of the overlying water (δ^{202}Hg = −0.67 ± 0.21‰, Δ^{199}Hg = 0.29 ± 0.38‰) in the investigated rice paddy during the same sampling periods were reported by Yin et al.[45] The enrichment factor for microbial reduction (ε^{202}Hg = −1.51 ± 0.24‰, E^{199}Hg = 0) was determined in Section 3.1. Previous experimental studies have shown that the range of isotopic enrichment factors for abiotic dark reduction under different conditions (ε^{202}Hg = −1.77 ∼ −1.52‰, E^{199}Hg = 0.17 ∼ 0.26‰[29]) was relatively small compared to that for photoreduction (ε^{202}Hg = −1.72 ∼ −0.60‰, E^{199}Hg = −6.73 ∼ −0.43‰[25,28,31]) and microbial reduction experiments (ε^{202}Hg = −2.00 ∼ −1.20‰[26,27]). Therefore, in this study, the enrichment factor for abiotic dark reduction was obtained from Zheng and Hintelmann.[29] The uncertainties in the enrichment factors for different reduction processes and the average Hg isotopic composition of the overlying water limit accurate calculations of the isotopic compositions of Hg(0) produced from different reduction processes. Therefore, Monte Carlo simulations were used here to quantify these uncertainties. As shown in Figure 3, the

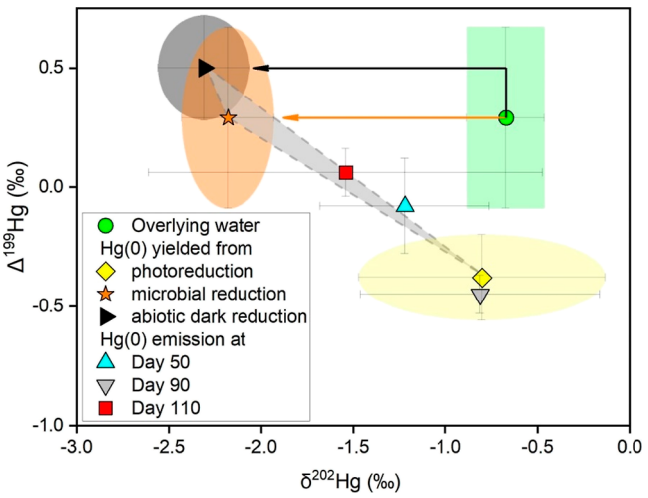

Figure 3. Hg isotopic compositions (Δ^{199}Hg vs. δ^{202}Hg) of Hg(0) exchanged between paddy soils and the atmosphere. Error bars indicate the 2SD analytical uncertainty. Arrows represent the enrichment processes from the overlying water to the endmembers (microbial reduction and abiotic dark reduction).

isotopic compositions of Hg(0) produced from microbial reduction (δ^{202}Hg = −2.18 ± 0.25‰, Δ^{199}Hg = 0.29 ± 0.38‰, 2SD) and abiotic dark reduction (δ^{202}Hg = −2.31 ± 0.25‰, Δ^{199}Hg = 0.50 ± 0.22‰, 2SD) were calculated using eqs S6 and S7 in Text S3. As described in Section 3.2, the isotopic compositions of Hg(0) produced from photoreduction (δ^{202}Hg = −0.80 ± 0.67‰, Δ^{199}Hg = −0.38 ± 0.18‰, 2SD) were measured in the rice paddy.

Based on a ternary mixing model, the relative contributions of different Hg(II) reduction processes associated with Hg(0) emissions from the rice paddy soil were evaluated using a Monte Carlo approach (Figure 4). Results showed that Hg(II) photoreduction, microbial reduction, and abiotic dark reduction contributed 62 ± 8, 18 ± 10, and 20 ± 13%,

https://doi.org/10.1021/acs.est.4c02143
Environ. Sci. Technol. 2024, 58, 11053−11062

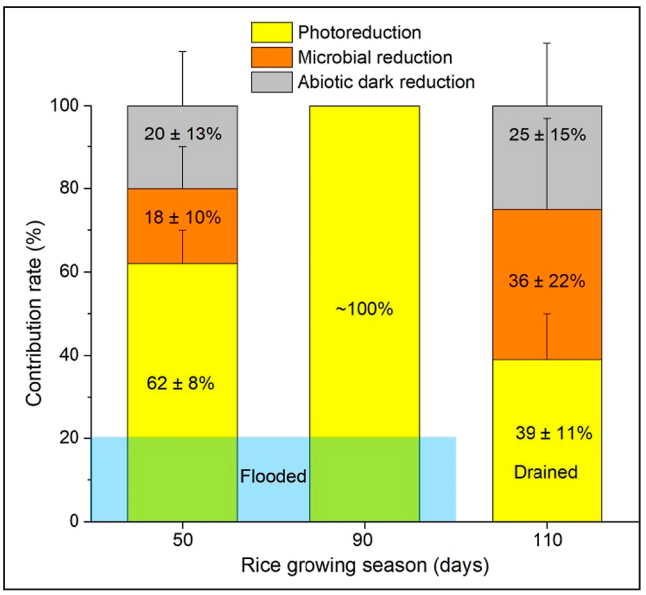

Figure 4. Contribution rates of three Hg(II) reduction processes to Hg(0) emissions from paddy soils at different sampling times.

respectively, to the total Hg(0) emission from the rice paddy soil on the 50th day, and were 39 ± 11, 36 ± 22, and 25 ± 15%, respectively, on the 110th day. However, on the 90th day, the contribution of photoreduction was nearly 100% since the average isotopic compositions of the emitted Hg(0) were very close to the photoreduction endmember, meaning the contributions of the other two nonphotoreduction processes were almost negligible. This may not imply that photoreduction was the only process during this period, but rather that the effect of photoreduction was significantly stronger than that of the other two reduction processes. Moreover, the average Hg(0) emission fluxes were significantly higher during day- than nighttime on both the 50 and 90th day (as presented in Section 3.3), possibly because the rate of photoreduction was significantly higher than that of nonphotoreduction.[49] However, on the 110th day, the contribution of photoreduction decreased due to the low penetration of solar radiation in dry paddy soils,[58] while the relative contributions of microbial reduction and abiotic dark reduction increased correspondingly.

In current chemical transport models assessing terrestrial Hg(0) emissions, natural emissions rarely separate different Hg(II) reduction processes.[13,59] Photoreduction is considered the primary process of Hg(0) emissions from natural surfaces,[13,14] while ignoring other Hg(II) reduction processes (e.g., microbial reduction and abiotic dark reduction) may underestimate Hg(0) emissions from natural surfaces. Our results indicated that photoreduction was indeed the dominant factor affecting the Hg(0) emission from paddy soils on the 90th day; however, the contributions of microbial reduction and abiotic dark reduction during other periods cannot be ignored, and these processes should be considered in future assessment of Hg(0) emissions from farmland soils and other land surfaces. In addition, higher photoreduction contributions and higher Hg(0) emission fluxes occurred during the flood stage when compared to the drainage period, suggesting that broader wetland ecosystems (approximately six times the area of global rice paddies,[18]) may be important natural Hg(0) sources, whereas wetlands have long been recognized as Hg(0) sinks.[60]

4. ENVIRONMENTAL IMPLICATIONS

The ranges of isotopic fractionation caused by Hg(II) reduction processes, especially photoreduction, obtained from in situ controlled experiments over a rice paddy soil were much smaller than previously reported values generated from laboratory-simulated experiments, probably due to different field and laboratory conditions or simultaneous Hg reduction and oxidation reactions. Although photoreduction is the dominant reduction pathway for Hg(0) emissions from paddy soils, microbial reduction and abiotic dark reduction pathways also contribute appreciable amounts of Hg(0) emissions under certain field conditions. Given that microbial reduction and abiotic dark reduction processes are widespread in natural environments, the contributions of these two reduction processes should be carefully considered when estimating inventories of Hg(0) emissions from natural sources to minimize uncertainties in Hg cycling assessments. In addition, stable isotope evidence has shown that atmosphere-foliage Hg(0) exchange is a bidirection exchange process and that foliage is a sink of atmospheric Hg(0).[61] However, rice plant-atmosphere Hg(0) exchange is currently unknown, and future work is needed to investigate the potential contribution of rice plants to the air-land exchange of Hg(0).

Although the rice paddy field used in this study is representative, the particularity of wet−dry alternation irrigation procedure of this type of field prevents the generalization of the results obtained from this study to other terrestrial landscapes. Therefore, future studies on the stable isotopic characteristics of Hg(0) emissions from different types of terrestrial landscapes and large water bodies are needed to provide additional field data for constraining the estimates of natural Hg(0) emissions and calibrating global Hg cycling models. In particular, data from wetlands and lakes, which have received large amounts of historically exogenous Hg from atmospheric deposition or runoff,[60] are noteworthy.

■ ASSOCIATED CONTENT

Supporting Information

The Supporting Information is available free of charge at https://pubs.acs.org/doi/10.1021/acs.est.4c02143.

Additional experimental details and additional figures (PDF)

■ AUTHOR INFORMATION

Corresponding Author

Bo Meng − *State Key Laboratory of Environmental Geochemistry, Institute of Geochemistry, Chinese Academy of Sciences, Guiyang 550081, China;* orcid.org/0000-0002-7827-8673; Phone: +86-851-84396920; Email: mengbo@vip.skleg.cn; Fax: +86-851-85891721

Authors

Kun Zhang − *State Key Laboratory of Environmental Geochemistry, Institute of Geochemistry, Chinese Academy of Sciences, Guiyang 550081, China; University of Chinese Academy of Sciences, Beijing 100049, China*

Qiang Pu − *State Key Laboratory of Environmental Geochemistry, Institute of Geochemistry, Chinese Academy of Sciences, Guiyang 550081, China*

https://doi.org/10.1021/acs.est.4c02143
Environ. Sci. Technol. 2024, 58, 11053−11062

Jiang Liu − *College of Resources, Sichuan Agricultural University, Chengdu 611130, China; State Key Laboratory of Environmental Geochemistry, Institute of Geochemistry, Chinese Academy of Sciences, Guiyang 550081, China*
Zhengdong Hao − *State Key Laboratory of Environmental Geochemistry, Institute of Geochemistry, Chinese Academy of Sciences, Guiyang 550081, China; University of Chinese Academy of Sciences, Beijing 100049, China*
Lijuan Zhang − *Key Laboratory for Heavy Metal Pollution Control and Reutilization, School of Environment and Energy, Peking University Shenzhen Graduate School, Shenzhen 518055, China;* orcid.org/0000-0002-5690-8005
Leiming Zhang − *Air Quality Research Division, Science and Technology Branch, Environment and Climate Change Canada, Toronto, Ontario M3H 5T4, Canada;* orcid.org/0000-0001-5437-5412
Xuewu Fu − *State Key Laboratory of Environmental Geochemistry, Institute of Geochemistry, Chinese Academy of Sciences, Guiyang 550081, China;* orcid.org/0000-0002-5174-7150
Xinbin Feng − *State Key Laboratory of Environmental Geochemistry, Institute of Geochemistry, Chinese Academy of Sciences, Guiyang 550081, China; University of Chinese Academy of Sciences, Beijing 100049, China;* orcid.org/0000-0002-7462-8998

Complete contact information is available at: https://pubs.acs.org/10.1021/acs.est.4c02143

Notes

The authors declare no competing financial interest.

■ ACKNOWLEDGMENTS

This research was supported by the National Natural Science Foundation of China (41931297) and the CAS "Light of West China" program. We greatly appreciate Prof. Peng Liang from Zhejiang Agriculture and Forestry University for kindly providing *G. sulfurreducens* PCA. We thank Dr. Fang Fang from Peking University Shenzhen Graduate School for her help in the pure culture experiment. We also thank Dr. Hongqian Yin and M.S. Qianshuo Zhang for providing assistance in sample collection and determination. We thank Prof. Runsheng Yin and Prof. Mingmin Cui for their edits and comments on the draft of this manuscript.

■ REFERENCES

(1) UNEP *Global Mercury Assessment 2018*; UN Environment Programme, Chemicals and Health Branch Geneva: Switzerland, 2019.
(2) Horowitz, H. M.; Jacob, D. J.; Zhang, Y.; Dibble, T. S.; Slemr, F.; Amos, H. M.; Schmidt, J. A.; Corbitt, E. S.; Marais, E. A.; Sunderland, E. M. A new mechanism for atmospheric mercury redox chemistry: implications for the global mercury budget. *Atmos. Chem. Phys.* **2017**, *17* (10), 6353−6371.
(3) Schroeder, W. H.; Munthe, J. Atmospheric mercury - An overview. *Atmos. Environ.* **1998**, *32* (5), 809−822.
(4) Wang, X.; Lin, C. J.; Yuan, W.; Sommar, J.; Zhu, W.; Feng, X. B. Emission-dominated gas exchange of elemental mercury vapor over natural surfaces in China. *Atmos. Chem. Phys.* **2016**, *16* (17), 11125−11143.
(5) Pirrone, N.; Cinnirella, S.; Feng, X.; Finkelman, R. B.; Friedli, H. R.; Leaner, J.; Mason, R.; Mukherjee, A. B.; Stracher, G. B.; Streets, D. G.; Telmer, K. Global mercury emissions to the atmosphere from anthropogenic and natural sources. *Atmos. Chem. Phys.* **2010**, *10* (13), 5951−5964.
(6) Song, S.; Selin, N. E.; Soerensen, A. L.; Angot, H.; Artz, R.; Brooks, S.; Brunke, E. G.; Conley, G.; Dommergue, A.; Ebinghaus, R.; Holsen, T. M.; Jaffe, D. A.; Kang, S.; Kelley, P.; Luke, W. T.; Magand, O.; Marumoto, K.; Pfaffhuber, K. A.; Ren, X.; Sheu, G. R.; Slemr, F.; Warneke, T.; Weigelt, A.; Weiss-Penzias, P.; Wip, D. C.; Zhang, Q. Top-down constraints on atmospheric mercury emissions and implications for global biogeochemical cycling. *Atmos. Chem. Phys.* **2015**, *15* (12), 7103−7125.
(7) Obrist, D.; Kirk, J. L.; Zhang, L.; Sunderland, E. M.; Jiskra, M.; Selin, N. E. A review of global environmental mercury processes in response to human and natural perturbations: Changes of emissions, climate, and land use. *Ambio* **2018**, *47* (2), 116−140.
(8) Outridge, P. M.; Mason, R. P.; Wang, F.; Guerrero, S.; Heimbürger-Boavida, L. E. Updated Global and Oceanic Mercury Budgets for the United Nations Global Mercury Assessment 2018. *Environ. Sci. Technol.* **2018**, *52* (20), 11466−11477.
(9) Yuan, W.; Wang, X.; Lin, C. J.; Wu, C. S.; Zhang, L. M.; Wang, B.; Sommar, J.; Lu, Z. Y.; Feng, X. B. Stable Mercury Isotope Transition during Postdepositional Decomposition of Biomass in a Forest Ecosystem over Five Centuries. *Environ. Sci. Technol.* **2020**, *54* (14), 8739−8749.
(10) O'Connor, D.; Hou, D.; Ok, Y. S.; Mulder, J.; Duan, L.; Wu, Q.; Wang, S.; Tack, F. M. G.; Rinklebe, J. Mercury speciation, transformation, and transportation in soils, atmospheric flux, and implications for risk management: A critical review. *Environ. Int.* **2019**, *126*, 747−761.
(11) Wang, S. F.; Feng, X. B.; Qiu, G. L.; Wei, Z. Q.; Xiao, T. F. Mercury emission to atmosphere from Lanmuchang Hg-Tl mining area, Southwestern Guizhou, China. *Atmos. Environ.* **2005**, *39* (39), 7459−7473.
(12) Zhu, J.; Wang, D.; Ma, M. Mercury release flux and its influencing factors at the air-water interface in paddy field in Chongqing. China. *Chin. Sci. Bull.* **2013**, *58* (2), 266−274.
(13) Smith-Downey, N. V.; Sunderland, E. M.; Jacob, D. J. Anthropogenic impacts on global storage and emissions of mercury from terrestrial soils: Insights from a new global model. *J. Geophys. Res.: Biogeosci.* **2010**, *115*, G03008.
(14) Zhang, Y. X.; Song, Z. C.; Huang, S. J.; Zhang, P.; Peng, Y. M.; Wu, P. P.; Gu, J.; Dutkiewicz, S.; Zhang, H. X.; Wu, S. L.; Wang, F. Y.; Chen, L.; Wang, S. X.; Li, P. Global health effects of future atmospheric mercury emissions. *Nat. Commun.* **2021**, *12* (1), 3035.
(15) Chen, C.; Huang, J.-H.; Li, K.; Osterwalder, S.; Yang, C.; Waldner, P.; Zhang, H.; Fu, X.; Feng, X. Isotopic Characterization of Mercury Atmosphere-Foliage and Atmosphere-Soil Exchange in a Swiss Subalpine Coniferous Forest. *Environ. Sci. Technol.* **2023**, *57* (42), 15892−15903.
(16) Jiskra, M.; Wiederhold, J. G.; Skyllberg, U.; Kronberg, R. M.; Hajdas, I.; Kretzschmar, R. Mercury Deposition and Re-emission Pathways in Boreal Forest Soils Investigated with Hg Isotope Signatures. *Environ. Sci. Technol.* **2015**, *49* (12), 7188−7196.
(17) Osterwalder, S.; Bishop, K.; Alewell, C.; Fritsche, J.; Laudon, H.; Åkerblom, S.; Nilsson, M. B. Mercury evasion from a boreal peatland shortens the timeline for recovery from legacy pollution. *Sci. Rep.* **2017**, *7* (1), 16022.
(18) Yoon, C. G. Wise use of paddy rice fields to partially compensate for the loss of natural wetlands. *Paddy Water Environ.* **2009**, *7* (4), 357−366.
(19) Chen, J.; Hu, G. R.; Liu, J.; Poulain, A. J.; Pu, Q.; Huang, R.; Meng, B.; Feng, X. B. The divergent effects of nitrate and ammonium application on mercury methylation, demethylation, and reduction in flooded paddy slurries. *J. Hazard. Mater.* **2023**, *460*, 132457.
(20) Liu, J.; Chen, J.; Poulain, A. J.; Pu, Q.; Hao, Z. D.; Meng, B.; Feng, X. B. Mercury and Sulfur Redox Cycling Affect Methylmercury Levels in Rice Paddy Soils across a Contamination Gradient. *Environ. Sci. Technol.* **2023**, *57* (21), 8149−8160.
(21) Wu, Q. Q.; Wang, B. L.; Hu, H. Y.; Bravo, A. G.; Bishop, K.; Bertilsson, S.; Meng, B.; Zhang, H.; Feng, X. B. Sulfate-reduction and

methanogenesis are coupled to Hg(II) and MeHg reduction in rice paddies. *J. Hazard. Mater.* **2023**, *460*, 132486.
(22) Blum, J. D.; Sherman, L. S.; Johnson, M. W. Mercury Isotopes in Earth and Environmental Sciences. *Annu. Rev. Earth Planet. Sci.* **2014**, *42* (1), 249−269.
(23) Kritee, K.; Motta, L. C.; Blum, J. D.; Tsui, M. T.-K.; Reinfelder, J. R. Photomicrobial Visible Light-Induced Magnetic Mass Independent Fractionation of Mercury in a Marine Microalga. *ACS Earth Space Chem.* **2018**, *2* (5), 432−440.
(24) Yin, R. S.; Feng, X. B.; Li, X. D.; Yu, B.; Du, B. Y. Trends and advances in mercury stable isotopes as a geochemical tracer. *Trends Environ. Anal. Chem.* **2014**, *2*, 1−10.
(25) Bergquist, B. A.; Blum, J. D. Mass-dependent and -independent fractionation of Hg isotopes by photoreduction in aquatic systems. *Science* **2007**, *318* (5849), 417−420.
(26) Kritee, K.; Blum, J. D.; Barkay, T. Mercury stable isotope fractionation during reduction of Hg(II) by different microbial pathways. *Environ. Sci. Technol.* **2008**, *42* (24), 9171−9177.
(27) Kritee, K.; Blum, J. D.; Johnson, M. W.; Bergquist, B. A.; Barkay, T. Mercury Stable Isotope Fractionation during Reduction of Hg(II) to Hg(0) by Mercury Resistant Microorganisms. *Environ. Sci. Technol.* **2007**, *41* (6), 1889−1895.
(28) Zheng, W.; Hintelmann, H. Mercury isotope fractionation during photoreduction in natural water is controlled by its Hg/DOC ratio. *Geochim. Cosmochim. Acta* **2009**, *73* (22), 6704−6715.
(29) Zheng, W.; Hintelmann, H. Nuclear Field Shift Effect in Isotope Fractionation of Mercury during Abiotic Reduction in the Absence of Light. *J. Phys. Chem. A* **2010**, *114* (12), 4238−4245.
(30) Motta, L. C.; Chien, A. D.; Rask, A. E.; Zimmerman, P. M. Mercury Magnetic Isotope Effect: A Plausible Photochemical Mechanism. *J. Phys. Chem. A* **2020**, *124* (19), 3711−3719.
(31) Rose, C. H.; Ghosh, S.; Blum, J. D.; Bergquist, B. A. Effects of ultraviolet radiation on mercury isotope fractionation during photoreduction for inorganic and organic mercury species. *Chem. Geol.* **2015**, *405*, 102−111.
(32) Zheng, W.; Hintelmann, H. Mass independent isotope fractionation of mercury during its photochemical reduction by low-molecular-weight organic compounds. *Geochim. Cosmochim. Acta* **2010**, *74* (12), A1224.
(33) Schwab, L.; Gallati, N.; Reiter, S. M.; Kimber, R. L.; Kumar, N.; McLagan, D. S.; Biester, H.; Kraemer, S. M.; Wiederhold, J. G. Mercury Isotope Fractionation during Dark Abiotic Reduction of Hg(II) by Dissolved, Surface-Bound, and Structural Fe(II). *Environ. Sci. Technol.* **2023**, *57* (40), 15243−15254.
(34) Wang, Y.; Bartov, G.; Wang, T.; Reinfelder, J. R.; Johnson, T. M.; Yee, N. Rapid Attainment of Isotopic Equilibrium after Mercury Reduction by Ferrous Iron Minerals and Isotopic Exchange between Hg(II) and Hg(0). *ACS Earth Space Chem.* **2021**, *5* (6), 1384−1394.
(35) Meng, B.; Feng, X.; Qiu, G.; Liang, P.; Li, P.; Chen, C.; Shang, L. The process of methylmercury accumulation in rice (Oryza sativa L.). *Environ. Sci. Technol.* **2011**, *45* (7), 2711−2717.
(36) Zhu, W.; Fu, X.; Zhang, H.; Liu, C.; Skyllberg, U.; Sommar, J.; Yu, B.; Feng, X. Mercury Isotope Fractionation during the Exchange of Hg(0) between the Atmosphere and Land Surfaces: Implications for Hg(0) Exchange Processes and Controls. *Environ. Sci. Technol.* **2022**, *56* (2), 1445−1457.
(37) Abdelhafiz, M. A.; Liu, J.; Jiang, T.; Pu, Q.; Aslam, M. W.; Zhang, K.; Meng, B.; Feng, X. DOM influences Hg methylation in paddy soils across a Hg contamination gradient. *Environ. Pollut.* **2023**, *322*, 121237.
(38) Ding, L. Y.; He, N. N.; Yang, S.; Zhang, L. J.; Liang, P.; Wu, S. C.; Wong, M. H.; Tao, H. C. Inhibitory effects of Skeletonema costatum on mercury methylation by Geobacter sulfurreducens PCA. *Chemosphere* **2019**, *216*, 179−185.
(39) Liu, Y. R.; Johs, A.; Bi, L.; Lu, X.; Hu, H. W.; Sun, D.; He, J. Z.; Gu, B. H. Unraveling Microbial Communities Associated with Methylmercury Production in Paddy Soils. *Environ. Sci. Technol.* **2018**, *52* (22), 13110−13118.
(40) Zhang, R.; Aris-Brosou, S.; Storck, V.; Liu, J.; Abdelhafiz, M. A.; Feng, X.; Meng, B.; Poulain, A. J. Mining-impacted rice paddies select for Archaeal methylators and reveal a putative (Archaeal) regulator of mercury methylation. *ISME Commun.* **2023**, *3* (1), 74.
(41) Hu, H.; Lin, H.; Zheng, W.; Rao, B.; Feng, X.; Liang, L.; Elias, D. A.; Gu, B. Mercury Reduction and Cell-Surface Adsorption by Geobacter sulfurreducens PCA. *Environ. Sci. Technol.* **2013**, *47* (19), 10922−10930.
(42) Zhang, W.; Sun, G. Y.; Yin, R. S.; Feng, X. B.; Yao, Z. X.; Fu, X. W.; Shang, L. H. Separation of methylmercury from biological samples for stable isotopic analysis. *J. Anal. At. Spectrom.* **2021**, *36* (11), 2415−2422.
(43) Gu, B. H.; Bian, Y. R.; Miller, C. L.; Dong, W. M.; Jiang, X.; Liang, L. Y. Mercury reduction and complexation by natural organic matter in anoxic environments. *Proc. Natl. Acad. Sci. U.S.A.* **2011**, *108* (4), 1479−1483.
(44) Richard, A.; Delvaux, J.; Bourel-Bonnet, L. Effects of sterilizing-grade filters on the physico-chemical properties of onion-like vesicles. *Int. J. Pharm.* **2006**, *312* (1−2), 144−150.
(45) Yin, H. Q.; Yao, H.; Yuan, W.; Lin, C. J.; Fu, X. W.; Yin, R. S.; Meng, B.; Luo, J.; Feng, X. B. Determination of the Isotopic Composition of Aqueous Mercury in a Paddy Ecosystem Using Diffusive Gradients in Thin Films. *Anal. Chem.* **2023**, *95* (33), 12290−12297.
(46) Yuan, W.; Wang, X.; Lin, C. J.; Sommar, J. O.; Wang, B.; Lu, Z. Y.; Feng, X. B. Quantification of Atmospheric Mercury Deposition to and Legacy Re-emission from a Subtropical Forest Floor by Mercury Isotopes. *Environ. Sci. Technol.* **2021**, *55* (18), 12352−12361.
(47) Fu, X.; Heimbürger, L. E.; Sonke, J. E. Collection of atmospheric gaseous mercury for stable isotope analysis using iodine- and chlorine-impregnated activated carbon traps. *J. Anal. At. Spectrom.* **2014**, *29*, 841−852.
(48) Huang, Q.; Liu, Y. L.; Chen, J. B.; Feng, X. B.; Huang, W. L.; Yuan, S. L.; Cai, H. M.; Fu, X. W. An improved dual-stage protocol to pre-concentrate mercury from airborne particles for precise isotopic measurement. *J. Anal. At. Spectrom.* **2015**, *30* (4), 957−966.
(49) Zhang, H.; Fu, X. W.; Wu, X.; Deng, Q. W.; Tang, K. H.; Zhang, L. M.; Sommar, J.; Sun, G. Y.; Feng, X. B. Using Mercury Stable Isotopes to Quantify Bidirectional Water-Atmosphere Hg(0) Exchange Fluxes and Explore Controlling Factors. *Environ. Sci. Technol.* **2023**, *57* (29), 10673−10685.
(50) USEPA. *Method 1631, Revision E: Mercury in Water by Oxidation, Purge and Trap, and Cold Vapor Atomic Fluorescence Spectrometry*; USEPA: Washington, DC, 2002.
(51) Yin, R. S.; Feng, X. B.; Foucher, D.; Shi, W. F.; Zhao, Z. Q.; Wang, J. High Precision Determination of Mercury Isotope Ratios Using Online Mercury Vapor Generation System Coupled with Multicollector Inductively Coupled Plasma-Mass Spectrometer. *Chin. J. Anal Chem.* **2010**, *38* (7), 929−934.
(52) Blum, J. D.; Bergquist, B. A. Reporting of variations in the natural isotopic composition of mercury. *Anal. Bioanal. Chem.* **2007**, *388* (2), 353−359.
(53) Estrade, N.; Carignan, J.; Sonke, J. E.; Donard, O. F. X. Measuring Hg Isotopes in Bio-Geo-Environmental Reference Materials. *Geostand. Geoanal. Res.* **2010**, *34* (1), 79−93.
(54) Wiederhold, J. G.; Cramer, C. J.; Daniel, K.; Infante, I.; Bourdon, B.; Kretzschmar, R. Equilibrium Mercury Isotope Fractionation between Dissolved Hg(II) Species and Thiol-Bound Hg. *Environ. Sci. Technol.* **2010**, *44* (11), 4191−4197.
(55) Zhang, L.; Wright, L. P.; Blanchard, P. A review of current knowledge concerning dry deposition of atmospheric mercury. *Atmos. Environ.* **2009**, *43* (37), 5853−5864.
(56) Fu, X. W.; Feng, X. B.; Yin, R. S.; Zhang, H. Diurnal variations of total mercury, reactive mercury, and dissolved gaseous mercury concentrations and water/air mercury flux in warm and cold seasons from freshwaters of southwestern China. *Environ. Toxicol. Chem.* **2013**, *32* (10), 2256−2265.

(57) Zhu, J. S.; Wang, D. Y.; Liu, X. A.; Zhang, Y. T. Mercury fluxes from air/surface interfaces in paddy field and dry land. *Appl. Geochem.* **2011**, *26* (2), 249−255.
(58) Fu, X. W.; Feng, X. B.; Zhang, H.; Yu, B.; Chen, L. G. Mercury emissions from natural surfaces highly impacted by human activities in Guangzhou province, South China. *Atmos. Environ.* **2012**, *54*, 185−193.
(59) Zhang, Y. X.; Zhang, P.; Song, Z. C.; Huang, S. J.; Yuan, T. F.; Wu, P. P.; Shah, V. R.; Liu, M. D.; Chen, L.; Wang, X. J.; Zhou, J.; Agnan, Y. An updated global mercury budget from a coupled atmosphere-land-ocean model: 40% more re-emissions buffer the effect of primary emission reductions. *One Earth* **2023**, *6* (3), 316−325.
(60) Zhang, J.; Li, C.; Tang, W.; Wu, M.; Chen, M.; He, H.; Lei, P.; Zhong, H. Mercury in wetlands over 60 years: Research progress and emerging trends. *Sci. Total Environ.* **2023**, *869*, 161862.
(61) Yuan, W.; Sommar, J.; Lin, C. J.; Wang, X.; Li, K.; Liu, Y.; Zhang, H.; Lu, Z. Y.; Wu, C. S.; Feng, X. B. Stable Isotope Evidence Shows Re-emission of Elemental Mercury Vapor Occurring after Reductive Loss from Foliage. *Environ. Sci. Technol.* **2019**, *53* (2), 651−660.

https://doi.org/10.1021/acs.est.4c02143
Environ. Sci. Technol. 2024, 58, 11053−11062